International Journal of Power Electronics and Drive Systems (IJPEDS)
Vol. 14, No. 4, December 2023, pp. 2307~2318
ISSN: 2088-8694, DOI: 10.11591/ijpeds.v14.i4.pp2307-2318

Design of the transmitter coil used in wireless power transfer system based on genetic algorithm

Mongkol Konghirun, Supapong Nutwong, Anawach Sangswang, Nattapong Hatchavanich
Department of Electrical Engineering, King Mongkut's University of Technology Thonburi, Bangkok, Thailand

Article Info

Article history:

Received Jan 11, 2023
Revised Apr 20, 2023
Accepted May 3, 2023

Keywords:

Circular flat spiral coil
Genetic Algorithm
Optimal design
System performance
Wireless power transfer

ABSTRACT

Performance of the wireless power transfer (WPT) system relies on the physical dimensions of the coupled coil, which should be optimally designed to meet required system performance and reduce the operating cost. This paper presents an optimal design based on genetic algorithm (GA) for the transmitter coil used in wireless power transfer system. Physical parameters of the circular flat spiral coil, including wire's cross-sectional area, coil's inner diameter, coil's outer diameter, coil's turn number, and space between each turn of the coil are considered. The design objective is to minimize the total wire length required by the coil subjected to both linear and nonlinear constraints. The design process is implemented on MATLAB optimization toolbox which is simple and accurate. The validity of proposed optimal coil design is verified by the experiment, which indicates that total wire length of the optimized coil can be reduced by 5.5 percent compared to the conventional coil without sacrificing the system performance. System efficiency obtained from the optimized coil can be improved up to 8.32 percent.

Corresponding Author:

Supapong Nutwong
Department of Electrical Engineering, King Mongkut's University of Technology Thonburi
126 Pracha Uthit Rd., Bang Mod, Thung Khru, Bangkok, 10140, Thailand
Email: supapong.nut@kmutt.ac.th

1. INTRODUCTION

Wireless power transfer (WPT) is an innovative technique that allows the electrical energy to transmit from source to load without any physical connection. It provides contactless, safety, convenient, and automated operation. Nowadays, it has been successfully adopted in various applications, such as implantable biomedical devices [1]–[3], portable devices [4]–[6], robot [7]–[9], kitchen appliances [10], electric vehicles (EVs) [11]–[14], electric bicycle [15]–[17], unmanned aerial vehicle [18]–[20], and IoT devices [21]–[25].

Since the working principle of WPT system is based on electromagnetic induction, the coupled coil, i.e., transmitter (Tx) and receiver (Rx) coil, are the most important part of this system. A circular flat spiral coil structure is frequently used as a coupled coils in the WPT system due to it is easy to fabricate and having scalable function [26]. Additionally, the magnetic coupling between coupled coils is radial symmetry where misalignment tolerance is the same in all directions [27]. Physical parameters of this coil structure, including cross-sectional area of litz-wire, inner diameter, outer diameter, number of turns, and space between each turn of the coil, have a significant impact on the performance of WPT system [28].

These parameters have been investigated in previous research efforts. The length of inner diameter of transmitter and receiver coil are considered which leads to the key design consideration as follows: i) The system will be less sensitive to misalignment if the inner diameter of transmitter coil is large; and ii) The average coupling factor increases with the inner diameter of a receiver coil [29]. The outer diameter is set to

constant at 300 mm, while the inner diameter and space between each turn of the coil are varied. It found that the ratio between inner diameter and outer diameter should be lower than or equal to 0.4 to achieve a relatively high coupling coefficient [30]. In addition, if the space between each turn is increased it will lower the coil's self-inductance, but it has less effect on the magnetic coupling coefficient. Five coupled coils with different dimensions are compared [31]. Physical parameters of a transmitter coil are fixed, but the inner diameter and outer diameter of the receiver coil are varied to investigate the coil pair that least sensitive to misalignments. From this finding, to obtain the coupled coil that is least sensitive to misalignment, it should be designed to meet the following guideline: i) The inner diameter of a receiver coil should be greater than the inner diameter of a transmitter coil; ii) The outer diameter of transmitter and receiver coils should be equal. The inner diameter, outer diameter, and number of turns are investigated to obtain the key design parameters that leads to high figure of merit (FOM), which is the product of magnetic coupling coefficient and system quality factor [32]. It is noted that system efficiency is directly proportional to this FOM. From various comparative studies, it leads to the design guideline to achieve a high value of FOM, which can be summarized as follows: i) Both transmitter and receiver coils should have the same number of turns. Moreover, the FOM increases with the coil turn numbers; ii) For a given number of turns and outer diameter, inner diameter should be as large as possible; iii) Since the outer diameter has less effect on the FOM, it should be fixed according to the applications. The inner diameter, outer diameter, and space between each turn of the coil (turn spacing) of the transmitter coil are investigated according to the following assumptions: i) Self-inductance of both transmitter and receiver coils are kept constant; ii) Wire diameter of both Tx and Rx coil are set to 4 mm; iii) Physical parameters of the receiver coil are fixed [33]. It was discovered that, while increasing the turn spacing, the system will be sensitive to misalignment if the outer diameter is kept constant. In contrast, the system will be less sensitive to misalignment if the inner diameter is kept constant. Four transmitter coils with different inner diameter, outer diameter, and number of turns are investigated to compare the transferred power, system efficiency, and required total wire length (TWL) [34]. The wire diameter and turn spacing of the Tx coil are fixed and the physical parameters of a receiver coil are set to constant. It can be concluded from this comparative study that the TWL will be lowest, and the transferred power will be highest if the inner diameter of Tx coil is greater than the inner diameter of Rx coil and the outer diameter of Tx coil is smaller than the outer diameter of Rx coil. Moreover, the mentioned Tx coil provides considerably high efficiency and is suitable to use at aligned position.

Unfortunately, the optimal physical parameters of a circular flat spiral coil structure have not been reported in the literature due to the complexity of optimizing the system with multi-variables. Thus, the optimization technique should be adopted in the design process of WPT coil. For a given output power, system efficiency is dependent on the self-inductance of a transmitter coil. To achieve high self-inductance, conventional Tx coil used in WPT system usually have small inner diameter and a lot of turn numbers. This increases the total wire length required by the coil which led to high cost and ohmic loss.

This paper presents an optimal design of the transmitter coil used in WPT system based on genetic algorithm. Inner diameter and number of turns of the circular flat spiral coil structure are optimized. The design objective is to minimize the total wire length required by the coil, while the design constraints are maximum outer diameter and minimum self-inductance. The presented optimal design is implemented on MATLAB optimization toolbox which is simple and accurate. The optimal design results are validated through an experiment where the total wire length and system efficiency are compared with the conventional coil. This paper is organized as follows: system description, analysis of the impact of self-inductance on system performance, and calculation of self-inductance of circular flat spiral coil are introduced in section 2. Implementation of the genetic algorithm using MATLAB simulation toolbox is presented in section 3. The experimental results and discussion are reported in section 4. The conclusion is detailed in section 5.

2. SYSTEM ANALYSIS

2.1. System description

The wireless power transfer system under studied is shown in Figure 1, which consists of DC voltage source, inverter circuit, transmitter coil, receiver coil, compensation capacitors, rectifier circuit, and a resistive load. Two coils configuration, i.e., one transmitter (Tx) and one receiver (Rx) coil, are adopted in this WPT system. Both Tx and Rx coils have a circular flat spiral coil structure. The mutual inductance between coupled coils is represented by "M". Compensation capacitors C_1 and C_2 are connected in series with Tx and Rx coil, respectively. This forms a series-series (S-S) compensation topology. The S-S topology is selected in this work because the system resonant frequency is insensitive to the mutual inductance variation which occur when there is misalignment between Tx and Rx coils [35]–[37]. Therefore, the fixed-frequency operation of an inverter circuit can be applied. A full-bridge inverter is adopted in the primary circuit to convert DC into high frequency AC voltage. Its switching frequency is fixed at resonant frequency

throughout the operation. The duty cycle of each switch is set to 50 percent which causes the inverter output voltage to be a square wave. An uncontrolled full-wave bridge rectifier is used in the secondary circuit to obtain a smooth DC voltage at the output. Load resistance is defined by "R_L". In this studied system, the output power is regulated by manually adjusting the magnitude of DC input voltage.

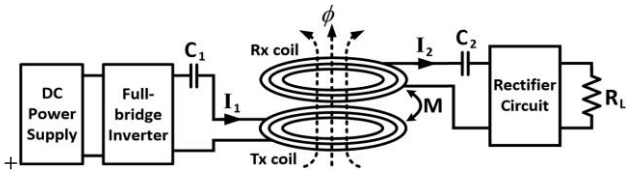

Figure 1. Wireless power transfer system under studied

2.2. Impact of self-inductance on system performance

Simplified equivalent circuit of WPT system under studied is shown in Figure 2 based on the mutual inductance coupling model. From the first harmonic approximation (FHA), the square wave voltage at an inverter output can be substituted by a sinusoidal voltage source (V_{in}). Self-inductance of transmitter coil and receiver coil are denoted by L_1 and L_2, respectively. A rectifier circuit and load resistor can be replaced by an equivalent AC resistance (R_{ac}) [38] as (1).

$$R_{ac} = \frac{8R_L}{\pi^2} \tag{1}$$

The system will be operated at resonant frequency (f_0) if compensation capacitances C_1 and C_2 are tuned to

$$C_1 = \frac{1}{4\pi^2 f_0^2 L_1} \tag{2}$$

$$C_2 = \frac{1}{4\pi^2 f_0^2 L_2} \tag{3}$$

at resonant frequency, the magnitude of secondary current (I_2) and output power (P_{out}) are derived as:

$$\left|\vec{I}_2\right| = \frac{2\pi f_0 k|\vec{I}_1|\sqrt{L_1 L_2}}{R_2+R_{ac}} \tag{4}$$

$$P_{out} = \frac{4R_{ac}L_1L_2\pi^2 f_0^2 k^2 \left|\vec{I}_1\right|^2}{2(R_2+R_{ac})^2} \tag{5}$$

where *k* is the magnetic coupling coefficient or coupling factor of a coupled coil. The impedance that reflects from secondary circuit to primary circuit is illustrated in Figure 3, which can be calculated by (6).

$$\vec{Z}_r = \frac{4L_1L_2\pi^2 f^2 k^2}{R_2+R_{ac}+j(2\pi f L_2 - 1/2\pi f C_2)} \tag{6}$$

This reflected impedance will be a purely resistive impedance at resonant frequency which is given as,

$$R_r = \frac{4L_1L_2\pi^2 f_0^2 k^2}{R_2+R_{ac}} \tag{7}$$

thus, the magnitude of primary current (I_1) can be obtained by (8),

$$\left|\vec{I}_1\right| = \frac{|\vec{V}_{in}|}{R_1+R_r} \tag{8}$$

where $\left|\vec{V}_{in}\right|$ is the magnitude of an input voltage. Substitute (8) into (5), the output power can be rewritten as (9).

$$P'_{out} = \frac{2R_{ac}L_1L_2\pi^2 f_0^2 k^2 \left|\vec{V}_{in}\right|^2}{(R_1+R_r)^2(R_2+R_{ac})^2} \tag{9}$$

The input power can be determined by (10).

$$P_{in} = \frac{|\vec{V}_{in}||\vec{I}_1|}{2} = \frac{|\vec{V}_{in}|^2}{2(R_1+R_r)} \quad (10)$$

The system efficiency can be evaluated from (9) and (10) as (11).

$$\eta = \frac{4R_{ac}L_1L_2\pi^2 f_0^2 k^2}{(R_1+R_r)(R_2+R_{ac})^2} \quad (11)$$

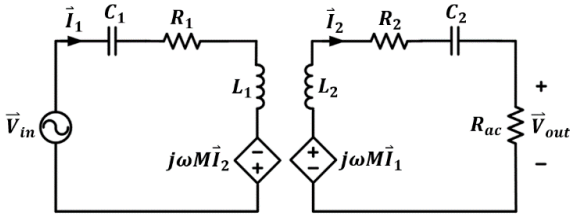

Figure 2. Simplified equivalent circuit of WPT system under studied

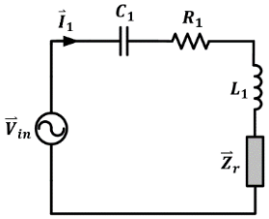

Figure 3. Reflected impedance in the primary circuit

For a given input voltage, resonant frequency, receiver coil, and a load, $|\vec{V}_{in}|$, f_0, L_2, R_2, and R_L are constant. Assuming the variation in self-inductance of transmitter coil (L_1) does not affect the k value, the reflected resistance (R_r) will be fixed. Therefore, the relationship between output power and self-inductance of Tx coil as in (9), and the relationship between system efficiency (η) and self-inductance L_1 as in (11) can be plotted as shown in Figures 4 and 5, respectively. It is clearly seen from Figures 4 and 5 that self-inductance of transmitter coil has a strong impact on the output power (P_{out}) and efficiency of WPT system. As noticed in Figure 4, the P_{out} is decreasing as the L_1 is increased, which is the inverse relationship. However, for a given self-inductance L_1, the output power can be boosted by adjusting the input voltage. For the same value of L_1, P_{out} will be increased if the coupling factor (k) is decreased. As pointed out in Figure 5, system efficiency is directly proportional to self-inductance of the Tx coil. Thus, to achieve better system efficiency compared to conventional transmitter coil, self-inductance of Tx coil (L_1) should be designed to be greater than the conventional one. In addition, for the same value of self-inductance L_1, system efficiency will be improved if the coupling factor (k) is increased.

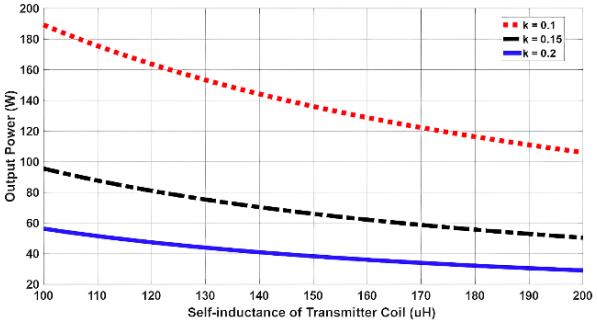

Figure 4. Output power as a function of self-inductance of Tx coil

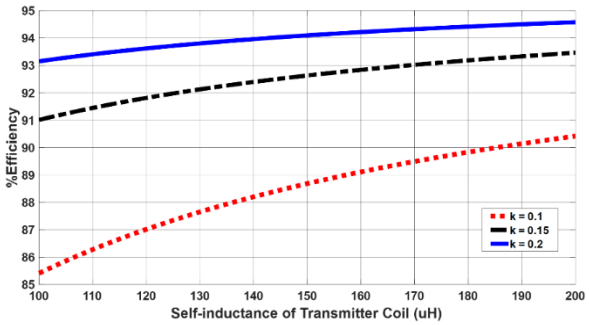

Figure 5. System efficiency as a function of self-inductance of Tx coil

2.3. Self-inductance of the circular flat spiral coil

A circular flat spiral coil structure used in the WPT system is shown in Figure 6, while its cross-sectional view is illustrated in Figure 7. Its self-inductance is dependent on the physical parameters of the coil, including cross-sectional area of litz-wire (w), inner diameter (d_i), outer diameter (d_o), number of turns (N), and space between each turn (s). The formular used for computing self-inductance of circular flat spiral coil corresponding to its physical parameters was first introduced in [39] which is expressed as (12).

$$L = \frac{a^2N^2}{8a+11c} \quad (12)$$

where $c = (d_o - d_i)/2$ and $a = (d_o + d_i)/4$. It is noted that the unit of calculated self-inductance in (12) is micro-Henry (μH) while the unit of inner diameter, outer diameter, and wire diameter are defined as inches.

Figure 6. Circular flat spiral coil structure used in WPT system

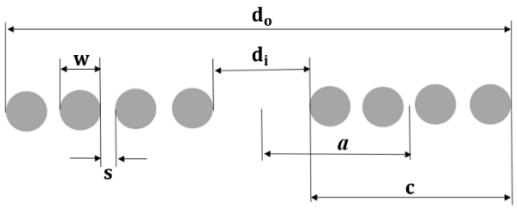

Figure 7. Cross-sectional view of the circular flat spiral coil structure

Let the space between each turn of the coil (s) is zero, "c" will be equal to "wN". Therefore, the self-inductance formular in (12) can be modified as in (13). It is noted in (13) that the unit of d_i, d_o, and w have been changed from inches to millimeters.

$$L' = \frac{(d_i+wN)^2N^2}{406.4d_i+1524wN} \quad (13)$$

As suggested in [39], the error of calculated self-inductance will be less than 5 percent if

$$0.9wN - 0.1d_i > 0 \quad (14)$$

total wire length (TWL) of the coil relies on its physical parameters, which can be computed by (15).

$$TWL = \sum_{k=1}^{N} 2\pi \left[\left(\frac{d_i+w}{2}\right) + (k-1)w\right] \quad (15)$$

3. GENETIC ALGORITHM

Genetic algorithm (GA) is the optimization algorithm which is developed from the biological evolution based on Charles Darwin's theory of natural selection. Key advantages of GA are the ability to deal with complex optimization problems. Although the GA can be implemented in any programming language, it requires a coding process which is complicated and time consuming. Nowadays, genetic algorithm can be realized on MATLAB optimization toolbox which is simple and accurate. It can be done by using the command in (16) where each attribute is defined in Table 1.

$$X = ga(FITNESSFCN, NVARS, A, b, Aeq, beq, lb, ub, NONLCON) \quad (16)$$

In this work, the optimal design of transmitter coil used in WPT system is performed based on GA which is implemented in MATLAB. The objective is to minimize the total wirelength of the coil as referred to (15). There are two design variables, which are inner diameter (d_i) and number of turns (N). The space between each turn (s) and diameter of litz-wire (w) are fixed at 0 and 3 mm, respectively. The minimum inner diameter and number of turns are set to 10 mm and 1 turn, which are the lower bound on design variables. The maximum inner diameter and number of turns are set to 200 mm and 50 turns, which are the upper bound on design variables. The outer diameter of the coil (d_o) is designed to not be bigger than 500 mm. This leads to a linear inequalities constraint which can be expressed as,

$$d_i + 2wN \leq 500 \quad (17)$$

The aim of optimal coil design presented in this paper is to reduce the total wirelength (TWL) required by the coil, and to enhance the system efficiency when compared to the conventional coil. The physical parameters of conventional coil are defined as listed in Table 2. Using (13), its calculated self-inductance is obtained as 113.83 μH. Thus, to ensure that the system efficiency obtained from optimized coil is higher than or equal to one obtained from conventional coil, self-inductance of the optimized coil must be

higher than or equal to 113.83 µH. This establishes a nonlinear inequalities constraint which can be derived as (18).

$$\frac{(d_i+wN)^2N^2}{406.4d_i+1524wN} \geq 113.83 \quad (18)$$

To limit the error of computed self-inductance within 5 percent, the condition in (14) should be included in the design process. Therefore, this condition will also be regarded as one of the nonlinear inequalities constraints. The value of all attributes in MATLAB's GA command are already introduced in Table 1. The optimization results are also presented in Table 2 where the global minimum of an objective function is met. As pointed out in Table 2, the total wirelength required by the optimized coil is reduced by 5.5 percent compared to the conventional coil, while the design variables satisfy all design constraints. This validates the presented optimal coil design.

Table 1. Definition and values of attributes in GA command

Attributes	Definition	Values
X	Design variables	d_i, N
FITNESSFCN	Fitness or objection function	$TWL = \sum_{k=1}^{N} 2\pi\left[\left(\frac{d_i+w}{2}\right)+(k-1)w\right]$
NVARS	Number of design variables	2
A, b	Linear inequalities constraints $(A \cdot X \leq b)$	$d_i + 2wN \leq 500$
Aeq, beq	Linear equalities constraints $(Aeq \cdot X = beq)$	-
lb	Lower bound on the design variables	10 mm, 1 turn
ub	Upper bound on the design variables	200 mm, 50 turns
NONLCON	Nonlinear constraints	$\frac{(d_i+wN)^2N^2}{406.4d_i+1524wN} \geq 113.83$ and $0.9wN - 0.1d_i > 0$

Table 2. Comparison between conventional coil and optimized coil

Parameters	Conventional coil	Optimized coil
Inner diameter (d_i)	20 mm	122 mm
Outer diameter (d_o)	230 mm	254 mm
Number of turns (N)	35 turns	22 turns
Space between each turn (s)	0 mm	0 mm
Diameter of litz-wire (w)	3 mm	3 mm
Self-inductance (L)	113.83 µH	113.92 µH
Total wire length (TWL)	13.74 m	12.99 m
$0.9wN - 0.1d_i$	92.5	47.2

4. EXPERIMENTAL RESULTS AND DISCUSSION

To verify the optimal design results, both conventional coil and optimized coil as indicated in Table 2 are fabricated, which are shown in Figure 8. The measured self-inductance and winding resistance of both conventional and optimized coils are presented in Table 3. Although there are some differences between calculation and measurement values of self-inductance, these errors are within 5 percent which complies with the condition discussed in (14). In traditional WPT system, physical dimensions of transmitter (Tx) and receiver (Rx) coils are identical. Thus, the dimensions of Rx coil used in this studied system will be the same as conventional coil.

For comparison purposes, both conventional and optimized Tx coils will be coupled with the same Rx coil. Figure 9 illustrates the comparison results of measured coupling factor between conventional and optimized Tx coil. The air gap (vertical distance) between Tx coil and Rx coil is fixed at 80 mm, while the Rx coil is horizontally moved from aligned position (0 mm) to 100 mm. The coupling factor obtained from conventional and optimized Tx coil at aligned position is almost equal, which are 0.213 and 0.218, respectively. When the horizontal misalignment between Tx coil and Rx coil is increased, the coupling factor obtained from both cases tends to decrease. However, when compared at the same misalignment, coupling factor of optimized Tx coil is greater than conventional Tx coil. It is noted that efficiency of WPT system increases with the coupling factor.

Table 3. Measured self-inductance and winding resistance of the fabricated coil

Parameters	Conventional coil	Optimized coil
Winding resistance	0.39	0.26
Self-inductance	117.46 µH	110.21 µH
Error between calculated and measured value of self-inductance	3.19%	-3.26%

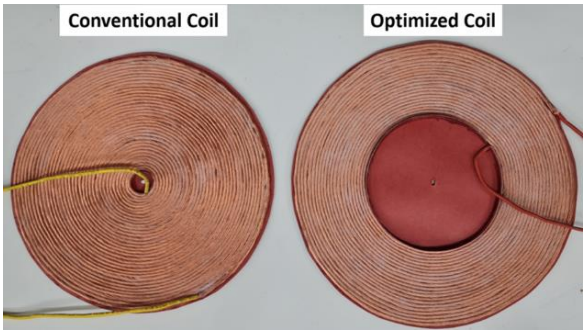

Figure 8. Fabricated coils under conventional and optimized parameters

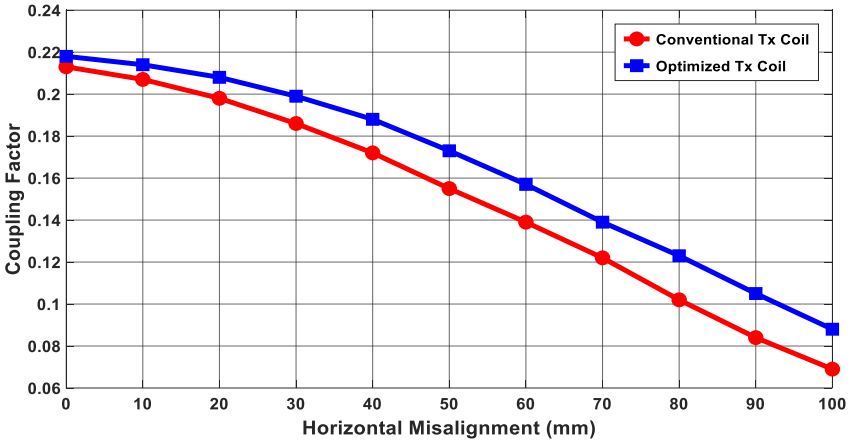

Figure 9. Comparison of measured coupling factor

To validate the presented optimal coil design, an experiment is performed on the 50-watt WPT system prototype which is shown in Figure 10. It is noted that the created experimental setup is for testing the presented concept. However, this proposed design can be applied to any of the static WPT applications. A benchtop DC power supply is used as the input DC voltage source. The full-bridge inverter circuit consists of four MOSFETs (IRFP460) and gate drive circuits. Its switching frequency (f_s) is fixed at 85 kHz throughout the operation, which is the system resonant frequency. An uncontrolled bridge rectifier circuit composes of four Schottky diode (SR3100) and filter capacitor (C_f). Film capacitors are used in the compensation capacitors (C_1 and C_2). Their capacitances are designed based on (2) and (3). Wire wound resistor is adopted as a resistive load (R_L). Circuit parameters of the created experimental set up are measured and listed in Table 4.

Table 4. Measured circuit parameters

Parameters	Values
C_1 (for conventional Tx coil)	30.22 µF
C_1 (for optimized Tx coil)	30.96 µF
C_2	30.22 µF
C_f	1,000 µF
R_L	12 Ω
f_s	85 kHz

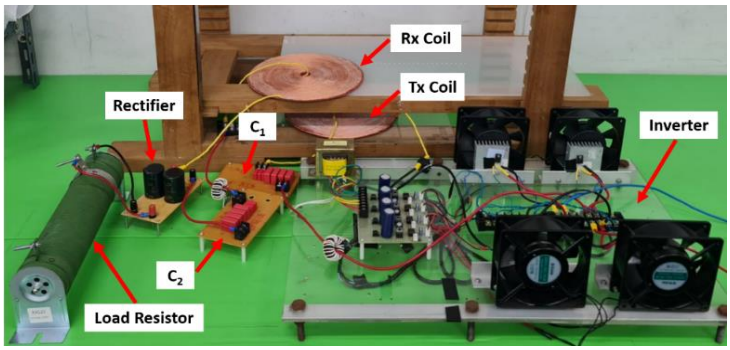

Figure 10. Experimental setup

Simplified equivalent circuit of the experimental set up is shown in Figure 11. An input DC voltage source is represented by V_{dc}. An inverter voltage and inverter current are denoted by I_{in} and V_{in}, respectively. A current passing through the receiver coil is defined as output current (I_{out}). The voltage at rectifier input is defined as output voltage (V_{out}).

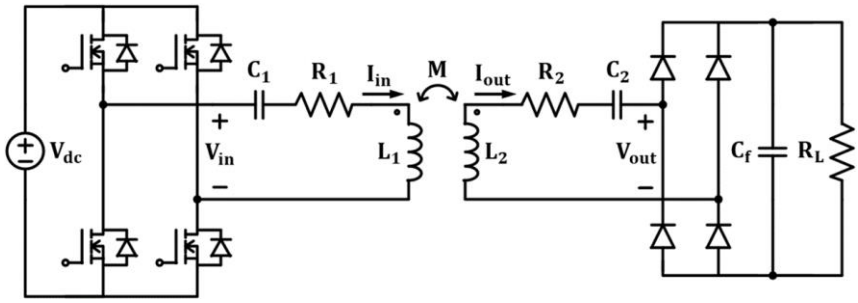

Figure 11. Simplified equivalent circuit of the experimental setup

Experimental waveforms of the studied system are measured using digital oscilloscope. The measurement is performed at 0 mm and 100 mm horizontal misalignment. To compare the efficiency obtained from conventional Tx coil and optimized Tx coil, the output power must be controlled to constant throughout the operation. Thus, it will be regulated to maintain at rated value of 50 watts by manually adjusting the magnitude of DC input voltage through a benchtop DC power supply. The input power (P_{in}) and output power (P_{out}) of the system are obtained from the average (mean) value of their instantaneous powers, which are the product between instantaneous voltage and instantaneous current. This can be done by using mathematical functions in digital oscilloscope.

At 0 mm horizontal misalignment, experimental results of the system with conventional Tx coil and optimized Tx coil are shown in Figures 12 and 13, respectively. As seen from the results, waveform of the voltage at an inverter output (V_{in}) is a square wave which has the frequency of 85 kHz. The current flowing in primary and secondary circuit, I_{in} and I_{out}, are sinusoid due to high-quality factor of the circuit. Since the capacitance of filter capacitor (C_f) is considerably high, the output voltage (V_{out}) is also a square wave. The current I_{in} is in phase with the voltage V_{in} while the current I_{out} is in phase with the voltage V_{out}. This is because the system operates in a resonant state. The measured output power (P_{out}) of each case is approximately equal to 50 watts. The measured input power (P_{in}) of conventional coil (56.531 W) is a little bit higher than optimized coil (56.1785 W). Therefore, efficiency of the system with optimized coil will be slightly greater than the system with conventional coil.

At 10 mm horizontal misalignment, experimental results of the system with conventional Tx coil and optimized Tx coil are shown in Figures 14 and 15, respectively. As seen from the results, waveform of the inverter voltage (V_{in}) is a square wave containing spike, which indicates the non-soft switching operation. This is because the inverter current (I_{in}) required to maintain the output power increases with the misalignment between Tx and Rx coils. Thus, the temperature of a coupled coil will rise which causes its self-inductance to decrease. As a result, system resonant frequency will be increased. Since the fixed

frequency operation is applied to this system, the switching frequency will be lower than the system resonant frequency. This forces the system to operate in non-ZVS region. Waveforms of the current flowing in primary and secondary circuit (I_{in} and I_{out}) remain the same, which are sinusoid. The output power (P_{out}) of both cases is approximately equal to 50 watts. Input power (P_{in}) of the system with optimized Tx coil is reduced by 5.35 watts or 7.7 percent compared to the system with conventional Tx coil. This improves the efficiency of the WPT system.

The measured system efficiency at different horizontal misalignment is shown in Figure 16 where the WPT system with conventional Tx coil is compared with the optimized Tx coil. At aligned position (0 mm), the measured efficiency of optimized Tx coil is 89.02 percent which is slightly higher than convention Tx coil (88.48 percent). When there is a horizontal misalignment between Tx and Rx coil, measured system efficiency obtained from both cases tend to decrease. However, system efficiency of optimized Tx coil is greater than conventional Tx coil for all the receiver coil positions. This agrees with the measured results of coupling factor. With the use of optimized Tx coil, system efficiency can be improved by 0.61 percent and 8.32 percent at 0 mm and 10 mm horizontal misalignment, respectively. The average increment of system efficiency of all horizontal misalignments (0 to 10 mm) is 2.43 percent.

The presented work is compared with the previous works in Table 5 where the physical parameters of circular flat spiral coil structure investigated in each work are summarized. These parameters have not been optimized in any previous work. In contrast, genetic algorithm is adopted in this work to design the optimal parameters of the coil which requires minimal total wire length. The presented work can be improved by including all physical parameters in the optimization process which will extend the feasibility of the presented optimal design.

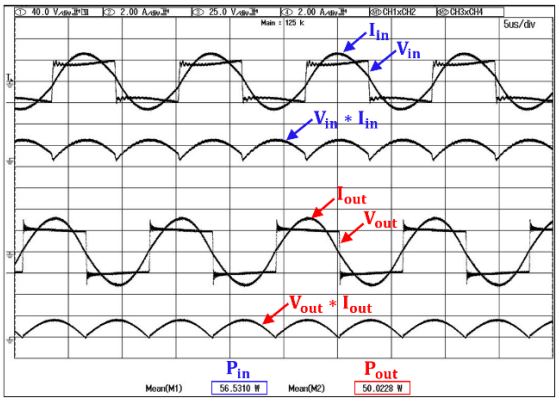

Figure 12. Experimental waveforms of the system with conventional Tx coil (0 mm misalignment)

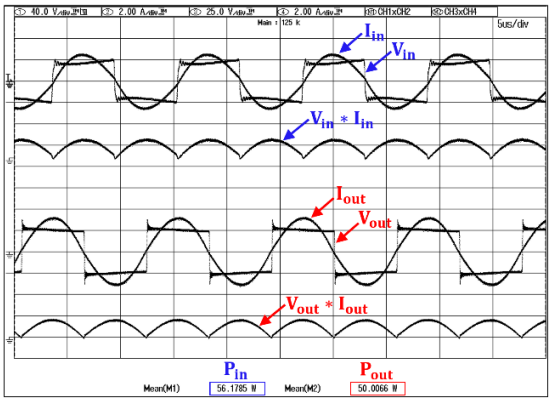

Figure 13. Experimental waveforms of the system with optimized Tx coil (0 mm misalignment)

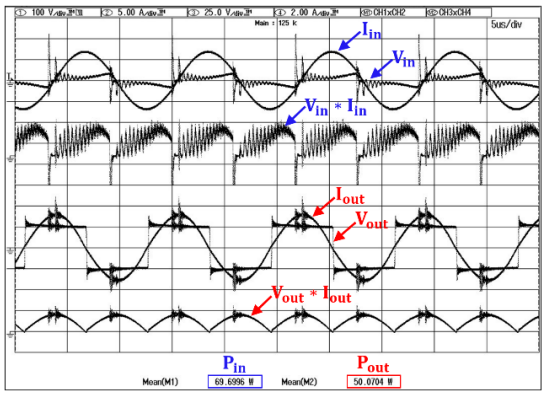

Figure 14. Experimental waveforms of the system with conventional Tx coil (10 mm misalignment)

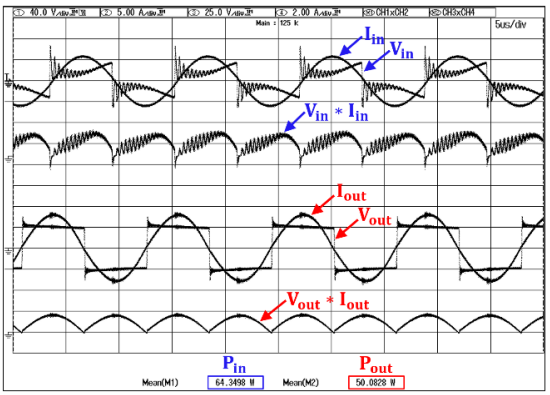

Figure 15. Experimental waveforms of the system with optimized Tx coil (0 mm misalignment)

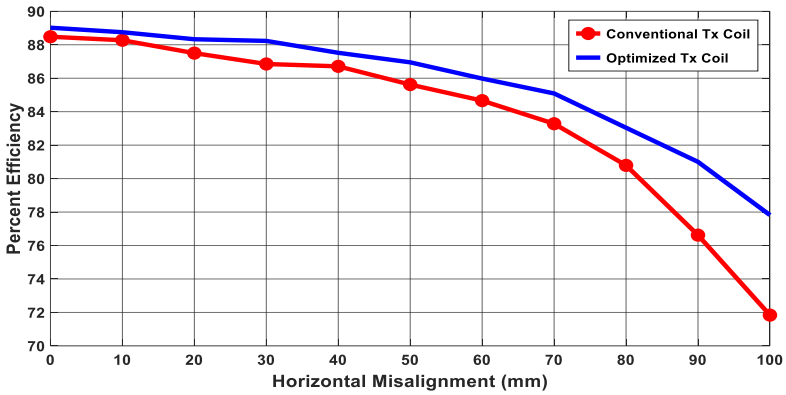

Figure 16. Comparison of measured system efficiency

Table 5. Comparison between presented work and previous works

Sources	Investigated parameters	Optimal design
[29]	Inner diameter	×
[30]	Inner diameter and turn spacing	×
[31]	Inner diameter and outer diameter	×
[32]	Inner diameter, outer diameter, and turn numbers	×
[33]	Inner diameter, outer diameter, and turn spacing	×
[34]	Inner diameter, outer diameter, and turn numbers	×
This work	Inner diameter and turn numbers	✓

5. CONCLUSION

The optimal design of transmitter coil used in wireless power transfer system is presented in this paper based on genetic algorithm. The design process is implemented in MATLAB optimization toolbox which is simple and accurate. Inner diameter and number of turns of circular flat spiral coil are optimized. The design objective is to minimize the total wirelength required by the coil, subjected to both linear and nonlinear constraints. The design results indicated that total wirelength of optimized coil can be decreased by 5.5 percent compared to conventional coil. This can reduce the cost and ohmic loss of WPT system. Furthermore, from the experimental measurement, the average increment of system efficiency is 2.43 percent with the use of optimized coil. In future work, the space between each turn of the coil and wire diameter will be included in the design variables to extend the feasibility of presented optimal design.

ACKNOWLEDGEMENTS

This research project is supported by Thailand Science Research and Innovation (TSRI). Basic Research Fund: Fiscal year 2022 under project number FRB650048/0164.

REFERENCES

[1] N. Ha-Van and C. Seo, "Modeling and experimental validation of a butterfly-shaped wireless power transfer in biomedical implants," *IEEE Access*, vol. 7, pp. 107225–107233, 2019, doi: 10.1109/ACCESS.2019.2933260.

[2] C. Xiao, S. Hao, D. Cheng, and C. Liao, "Safety enhancement by optimizing frequency of implantable cardiac pacemaker wireless charging system," *IEEE Transactions on Biomedical Circuits and Systems*, vol. 16, no. 3, pp. 372–383, Jun. 2022, doi: 10.1109/TBCAS.2022.3170575.

[3] B. Ouacha, H. Bouyghf, M. Nahid, and S. Abenna, "DEA-based on optimization of inductive coupling for powering implantable biomedical devices," *International Journal of Power Electronics and Drive Systems (IJPEDS)*, vol. 13, no. 3, p. 1558, Sep. 2022, doi: 10.11591/ijpeds.v13.i3.pp1558-1567.

[4] J. Wang *et al.*, "A conformal split-ring loop as a self-resonator for wireless power transfer," *IEEE Access*, vol. 8, pp. 911–919, 2020, doi: 10.1109/ACCESS.2019.2918640.

[5] H. Le-Huu and C. Seo, "Dual-band free-positioning transmitting coil for multiple-receiver wireless power transfer," *IEEE Access*, vol. 9, pp. 107298–107308, 2021, doi: 10.1109/ACCESS.2021.3101635.

[6] Q. Liu, M. Xiong, M. Liu, Q. Jiang, W. Fang, and Y. Bai, "Charging a smartphone over the air: the resonant beam charging method," *IEEE Internet of Things Journal*, vol. 9, no. 15, pp. 13876–13885, Aug. 2022, doi: 10.1109/JIOT.2022.3142031.

[7] Z. Zhang and B. Zhang, "Omnidirectional and efficient wireless power transfer system for logistic robots," *IEEE Access*, vol. 8, pp. 13683–13693, 2020, doi: 10.1109/ACCESS.2020.2966225.

[8] A. Sarin and A.-T. Avestruz, "Code division multiple access wireless power transfer for energy sharing in heterogenous robot swarms," *IEEE Access*, vol. 8, pp. 132121–132133, 2020, doi: 10.1109/ACCESS.2020.3010202.

[9] V. Krithika *et al*., "Wireless power transmission of mobile robot for target tracking," *International Journal of Power Electronics and Drive Systems (IJPEDS)*, vol. 13, no. 3, p. 1588, Sep. 2022, doi: 10.11591/ijpeds.v13.i3.pp1588-1598.
[10] S. Nutwong, A. Sangswang, S. Naetiladdanon, and E. Mujjalinvimut, "A novel output power control of wireless powering kitchen appliance system with free-positioning feature," *Energies*, vol. 11, no. 7, p. 1671, Jun. 2018, doi: 10.3390/en11071671.
[11] A. Mahesh, B. Chokkalingam, and L. Mihet-Popa, "Inductive wireless power transfer charging for electric vehicles–a review," *IEEE Access*, vol. 9, pp. 137667–137713, 2021, doi: 10.1109/ACCESS.2021.3116678.
[12] N. Hatchavanich, A. Sangswang, and M. Konghirun, "Secondary-side voltage control via primary-side controller for wireless EV chargers," *IEEE Access*, vol. 8, pp. 203543–203554, 2020, doi: 10.1109/ACCESS.2020.3036542.
[13] D. Baros, N. Rigogiannis, P. Drougas, D. Voglitsis, and N. P. Papanikolaou, "Transmitter side control of a wireless EV charger employing IoT," *IEEE Access*, vol. 8, pp. 227834–227846, 2020, doi: 10.1109/ACCESS.2020.3045803.
[14] A. F. A. Aziz, M. F. Romlie, and T. Z. A. Zulkifli, "CLL/S detuned compensation network for electric vehicles wireless charging application," *International Journal of Power Electronics and Drive Systems (IJPEDS)*, vol. 10, no. 4, p. 2173, Dec. 2019, doi: 10.11591/ijpeds.v10.i4.pp2173-2181.
[15] N. T. Diep, N. K. Trung, and T. T. Minh, "Wireless charging system for electric bicycle application," *International Journal of Power Electronics and Drive Systems (IJPEDS)*, vol. 11, no. 4, p. 1926, Dec. 2020, doi: 10.11591/ijpeds.v11.i4.pp1926-1935.
[16] H. Z. Z. Beh, G. A. Covic, and J. T. Boys, "Investigation of magnetic couplers in bicycle kickstands for wireless charging of electric bicycles," *IEEE Journal of Emerging and Selected Topics in Power Electronics*, vol. 3, no. 1, pp. 87–100, Mar. 2015, doi: 10.1109/JESTPE.2014.2325866.
[17] C.-C. Liao, M.-S. Huang, Z.-F. Li, F.-J. Lin, and W.-T. Wu, "Simulation-assisted design of a bidirectional wireless power transfer with circular sandwich coils for e-bike sharing system," *IEEE Access*, vol. 8, pp. 110003–110017, 2020, doi: 10.1109/ACCESS.2020.3000564.
[18] K. K. Hasan, S. Saat, Y. Yusop, and M. R. Awal, "Development of self-charging unmanned aerial vehicle system using inductive approach," *International Journal of Power Electronics and Drive Systems (IJPEDS)*, vol. 13, no. 3, p. 1635, Sep. 2022, doi: 10.11591/ijpeds.v13.i3.pp1635-1644.
[19] S. Wu, C. Cai, X. Liu, W. Chai, and S. Yang, "Compact and free-positioning omnidirectional wireless power transfer system for unmanned aerial vehicle charging applications," *IEEE Transactions on Power Electronics*, vol. 37, no. 8, pp. 8790–8794, Aug. 2022, doi: 10.1109/TPEL.2022.3158610.
[20] S. Wu, C. Cai, L. Jiang, J. Li, and S. Yang, "Unmanned aerial vehicle wireless charging system with orthogonal magnetic structure and position correction aid device," *IEEE Transactions on Power Electronics*, vol. 36, no. 7, pp. 7564–7575, Jul. 2021, doi: 10.1109/TPEL.2020.3047384.
[21] Z. Dai, Z. Fang, H. Huang, Y. He, and J. Wang, "Selective omnidirectional magnetic resonant coupling wireless power transfer with multiple-receiver system," *IEEE Access*, vol. 6, pp. 19287–19294, 2018, doi: 10.1109/ACCESS.2018.2809797.
[22] L. Wang, H. Shao, J. Li, X. Wen, and Z. Lu, "Optimal multi-user computation offloading strategy for wireless powered sensor networks," *IEEE Access*, vol. 8, pp. 35150–35160, 2020, doi: 10.1109/ACCESS.2020.2967559.
[23] H. Wu, H. Tian, G. Nie, and P. Zhao, "Wireless powered mobile edge computing for industrial internet of things systems," *IEEE Access*, vol. 8, pp. 101539–101549, 2020, doi: 10.1109/ACCESS.2020.2995649.
[24] H.-S. Lee and J.-W. Lee, "Adaptive wireless power transfer beam scheduling for non-static iot devices using deep reinforcement learning," *IEEE Access*, vol. 8, pp. 206659–206673, 2020, doi: 10.1109/ACCESS.2020.3037323.
[25] J. H. Park, N. M. Tran, S. Il Hwang, D. I. Kim, and K. W. Choi, "Design and implementation of 5.8 GHz RF wireless power transfer system," *IEEE Access*, vol. 9, pp. 168520–168534, 2021, doi: 10.1109/ACCESS.2021.3138221.
[26] M. Budhia, G. A. Covic, and J. T. Boys, "Design and optimization of circular magnetic structures for lumped inductive power transfer systems," *IEEE Transactions on Power Electronics*, vol. 26, no. 11, pp. 3096–3108, Nov. 2011, doi: 10.1109/TPEL.2011.2143730.
[27] E. Chaidee, A. Sangswang, S. Naetiladdanon, and S. Nutwong, "An inverter topology for multi transmitter wireless power transfer systems," *IEEE Access*, vol. 10, pp. 36592–36605, 2022, doi: 10.1109/ACCESS.2022.3162906.
[28] X. Liu, C. Xia, and X. Yuan, "Study of the circular flat spiral coil structure effect on wireless power transfer system performance," *Energies*, vol. 11, no. 11, p. 2875, Oct. 2018, doi: 10.3390/en11112875.
[29] C. Zheng, H. Ma, J.-S. Lai, and L. Zhang, "Design considerations to reduce gap variation and misalignment effects for the inductive power transfer system," *IEEE Transactions on Power Electronics*, vol. 30, no. 11, pp. 6108–6119, Nov. 2015, doi: 10.1109/TPEL.2015.2424893.
[30] Y. Wang, W. Liu, and Y. Xie, "Design and optimization for circular planar spiral coils in wireless power transfer system," in *2019 22nd International Conference on Electrical Machines and Systems (ICEMS)*, Aug. 2019, pp. 1–4, doi: 10.1109/ICEMS.2019.8922255.
[31] K. Aditya, V. K. Sood, and S. S. Williamson, "Magnetic characterization of unsymmetrical coil pairs using Archimedean spirals for wider misalignment tolerance in IPT systems," *IEEE Transactions on Transportation Electrification*, vol. 3, no. 2, pp. 454–463, Jun. 2017, doi: 10.1109/TTE.2017.2673847.
[32] K. Aditya, M. Youssef, and S. S. Williamson, "Design considerations to obtain a high figure of merit in circular archimedean spiral coils for EV battery charging applications," in *IECON 2015 - 41st Annual Conference of the IEEE Industrial Electronics Society*, Nov. 2015, pp. 005396–005401, doi: 10.1109/IECON.2015.7392949.
[33] Wenjing Li, Jianghua Lu, Bo Li, Guorong Zhu, and Wu Chen, "Impact of the wire tightness degree on circular pad with different coil size in IPT system," in *2017 IEEE 3rd International Future Energy Electronics Conference and ECCE Asia (IFEEC 2017 - ECCE Asia)*, Jun. 2017, pp. 2273–2278, doi: 10.1109/IFEEC.2017.7992406.
[34] S. Nutwong, E. Mujjalinvimut, T. Tricharoenlap, K. Siripatcharaphan, and W. Thaewjan, "Comparison of figure of merit of different circular coil used in inductive power transfer system," in *2021 9th International Electrical Engineering Congress (iEECON)*, Mar. 2021, pp. 169–172, doi: 10.1109/iEECON51072.2021.9440349.
[35] H. Li, J. Li, K. Wang, W. Chen, and X. Yang, "A Maximum efficiency point tracking control scheme for wireless power transfer systems using magnetic resonant coupling," *IEEE Transactions on Power Electronics*, vol. 30, no. 7, pp. 3998–4008, Jul. 2015, doi: 10.1109/TPEL.2014.2349534.
[36] X. del T. García, J. Vázquez, and P. Roncero-Sánchez, "Design, implementation issues and performance of an inductive power transfer system for electric vehicle chargers with series–series compensation," *IET Power Electronics*, vol. 8, no. 10, pp. 1920–1930, Oct. 2015, doi: 10.1049/iet-pel.2014.0877.
[37] J. Liu, Y. Zhang, Z. Wang, and M. Cheng, "Design of a high-efficiency wireless charging system for electric vehicle," in *2018 1st Workshop on Wide Bandgap Power Devices and Applications in Asia (WiPDA Asia)*, May 2018, pp. 40–44, doi: 10.1109/WiPDAAsia.2018.8734657.

[38] G. Guidi and J. A. Suul, "Minimizing converter requirements of inductive power transfer systems with constant voltage load and variable coupling conditions," *IEEE Transactions on Industrial Electronics*, vol. 63, no. 11, pp. 6835–6844, Nov. 2016, doi: 10.1109/TIE.2016.2582459.
[39] H. A. Wheeler, "Simple inductance formulas for radio coils," *Proceedings of the IRE*, vol. 16, no. 10, pp. 1398–1400, Oct. 1928, doi: 10.1109/JRPROC.1928.221309.

BIOGRAPHIES OF AUTHORS

Mongkol Konghirun is a lecturer in Electrical Engineering Department, Faculty of Engineering, King Mongkut's University of Technology Thonburi (KMUTT), Bangkok, Thailand; He received the B.Eng. degree (First Class Honors) in Electrical Engineering from the King Mongkut's University of Technology Thonburi in 1995; and the M.Sc. and Ph.D. degrees in Electrical Engineering from The Ohio State University, Columbus, OH, USA, in 1999 and 2003, respectively. Presently, he is an Associate Professor with the Department of Electrical Engineering, King Mongkut's University of Technology Thonburi. His research interests include electric motor drives, power electronics, railway electrification, and renewable energy. He can be contacted at email: mongkol.kon@kmutt.ac.th.

Supapong Nutwong is a lecturer in Electrical Engineering Department, Faculty of Engineering, King Mongkut's University of Technology Thonburi (KMUTT), Bangkok, Thailand since 2020; He received the B.Eng. degree and M.Eng. degree in Electrical Engineering from the King Mongkut's University of Technology Thonburi in 2007 and 2011, respectively; and the D.Eng. degree in Electrical and Information Engineering Technology from the King Mongkut's University of Technology Thonburi in 2019. From 2013 to 2014, he was a Researcher at the Educational Support Unit, KMUTT. Since 2022, he has been an Assistant Professor with the Department of Electrical Engineering, KMUTT. His research interests include the field of power electronics, inductive power transfer (IPT) systems, capacitive power transfer (CPT) systems, wireless charging applications, and induction heating systems. He can be contacted at email: supapong.nut@kmutt.ac.th.

Anawach Sangswang is a lecturer in Electrical Engineering Department, Faculty of Engineering, King Mongkut's University of Technology Thonburi (KMUTT), Bangkok, Thailand; He received the B.Eng. degree in Electrical Engineering from the King Mongkut's University of Technology Thonburi in 1995; and the M.Sc. and Ph.D. degrees in Electrical Engineering from Drexel University, Philadelphia, PA, in 1999 and 2003, respectively. Since 2020, he has been an Associate Professor with the Department of Electrical Engineering, KMUTT. From 1999 to 2003, he was a Research Assistant with the Center for Electric Power Engineering, Drexel University. His research interests include induction heating, wireless power transfer, energy management systems, and power system stability. He can be contacted at email: anawach.san@kmutt.ac.th.

Nattapong Hatchavanich is a lecturer in Electrical Engineering Department, Faculty of Engineering, King Mongkut's University of Technology Thonburi (KMUTT), Bangkok, Thailand since 2021; He received the B.Eng. degree in Electrical Engineering from the King Mongkut's University of Technology North Bangkok (KMUTNB) in 2012; received the M.Eng. degree in Electrical Engineering from the King Mongkut's University of Technology Thonburi in 2016; and the D.Eng. degree in Electrical and Information Engineering Technology from the King Mongkut's University of Technology Thonburi in 2020. His current research interests include the resonant inverter and control technique for wireless power transfer system (WPT) and induction heating applications. He can be contacted at email: nattapong.hat@kmutt.ac.th.